Stress transfer and strain rate variations during the seismic cycle

H. Perfettini
Institut de Recherche pour le Développement/Laboratoire des Mécanismes de Transferts en Géologie, Toulouse, France

J.-P. Avouac
Geological and Planetary Science Division, California Institute of Technology, Pasadena, California, USA

Received 28 November 2003; revised 15 March 2004; accepted 10 May 2004; published 22 June 2004.

[1] The balance of forces implies stress transfers during the seismic cycle between the elastobrittle upper crust and the viscoelastic lower crust. This could induce observable time variations of crustal straining in the interseismic period. We simulate these variations using a one-dimensional system of springs, sliders, and dashpot loaded by a constant force. The seismogenic zone and the zone of afterslip below are modeled from rate-and-state friction. The ductile deeper fault zone is modeled from a viscous slider with Newtonian viscosity ν. The force per unit length, F, must exceed a critical value F_c to overcome friction resistance of the fault system. This simple system produces periodic earthquakes. The recurrence period, T_{cycle}, and the duration of the postseismic relaxation phase, which is driven dominantly by afterslip, then both scale linearly with ν. Between two earthquakes, interseismic strain buildup across the whole system is nonstationary with the convergence rates V_i, just after each earthquake, being systematically higher than the value V_f at the end of the interseismic period. We show that V_i/V_f is an exponential function of $\alpha = T_{\text{cycle}}/T_{\text{M}} \propto \Delta\tau/(F - F_c) \propto \Delta\tau/(\nu V_0)$, where $\Delta\tau$ is the coseismic stress drop and V_0 is the long-term fault slip rate. It follows that departure from stationary strain buildup is higher if the contribution of viscous forces to the force balance is small compared to the coseismic stress drop (due to a low viscosity or low convergence rate, for example). This simple model is meant to show that the far-field deformation rate in the interseismic period, which can be determined from geodetic measurements, might not necessarily be uniform and equal to the long-term geologic rate. *INDEX TERMS:* 1242 Geodesy and Gravity: Seismic deformations (7205); 1236 Geodesy and Gravity: Rheology of the lithosphere and mantle (8160); 7230 Seismology: Seismicity and seismotectonics; 7215 Seismology: Earthquake parameters; 7209 Seismology: Earthquake dynamics and mechanics; *KEYWORDS:* earthquake cycle, postseismic relaxation, GPS

Citation: Perfettini, H., and J.-P. Avouac (2004), Stress transfer and strain rate variations during the seismic cycle, *J. Geophys. Res.*, *109*, B06402, doi:10.1029/2003JB002917.

1. Introduction

[2] Most models of the seismic cycle [e.g., *Savage and Prescott*, 1978; *Tse and Rice*, 1986; *Stuart*, 1988; *Lapusta and Rice*, 2003; *Mitsui and Hirahara*, 2001] are based on the assumption that at some distance from the fault, velocities are imposed by plates motion and do not vary with time. This assumption implicitly requires that tectonic forces in the far field build up gradually during the interseismic period. It might alternatively be contested that tectonic forces which primarily result from the distribution of mass and from dynamic forces induced by convection at large scale should rather be considered constant. If stress fluctuations away from the fault zone are negligibly small compared to the average ambient tectonic stresses, the two viewpoints are equivalent. This might not always be true, however, since some authors have shown that the regional stress field in the vicinity of a major megathrust might vary dramatically during the seismic cycle [e.g., *Dmowska et al.*, 1996]. In this paper we investigate the consequences of the hypothesis of a constant tectonic loading force on the seismic cycle. We consider the particular case of a megathrust modeled from a simple one-dimensional (1-D) system of springs and sliders (Figure 1). Although the model is obviously an oversimplification of reality, we believe it gives some insight into one mechanism by which deformation rate, even at some distance from the fault, might not be uniform in the interseismic period and could differ from long-term deformation rate.

[3] Hereafter we first present the simplified fault model assumed in the numerical simulations. We next discuss the characteristic of the earthquake cycle generated from this

0148-0227/04/2003JB002917$09.00

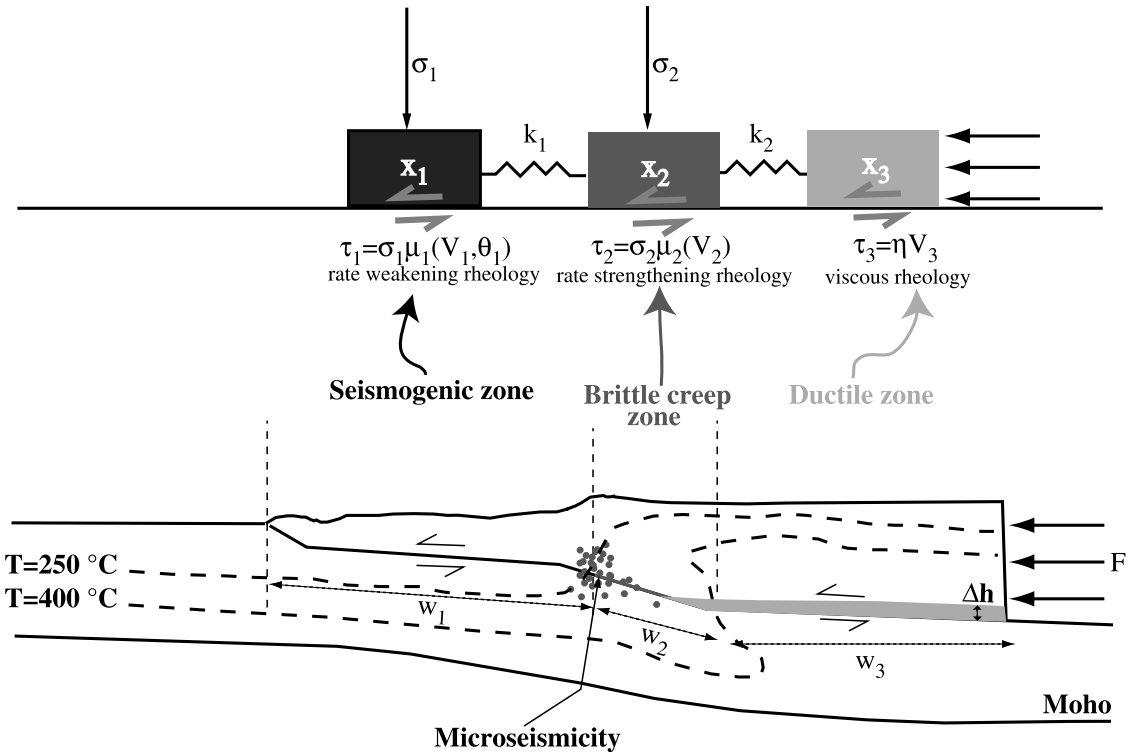

Figure 1. Fault model and 1-D springs and sliders model used in this study (see text for discussion).

model, focusing on the role played by viscous deformation on temporal variation of interseismic straining.

2. Fault Model

[4] The fault model was inspired by the case of intracontinental megathrust faults such as along the Himalaya or the central range in Taiwan [*Perfettini and Avouac*, 2004], but we believe it might apply more generally to any kind of megathrust. The variation of fault properties with depth is a standard representation that was inspired from field observations and rock mechanics experiments [e.g., *Scholz*, 1990; *Blanpied et al.*, 1991; *Wang*, 1995]. The seismogenic fault zone (SFZ), where temperature is less than $\simeq$250°C, is assumed to be brittle and to undergo stick slip due to rate-weakening frictional sliding. At depth, where temperature gets higher than ~400°C, it roots into the ductile fault zone (DFZ), supposedly governed by dislocation creep [*Cattin and Avouac*, 2000]. Between these two domains, the brittle creep fault zone (BCFZ) is assumed to obey rate-strengthening brittle creep. Between slip events the seismogenic fault zone is locked, and the convergence rate V_0 is absorbed by ductile shear along the DFZ at depth and elastic straining of brittle crust. When it slips, the stress drop has to be compensated by some stress increase on the deeper fault portion leading to some temporal variation of deformation. We have adopted a spring-and-slider modeling approach because it is the simplest way to account for these stress transfers during the seismic cycle and it is easily amenable to analytical analysis [*Burridge and Knopoff*, 1967]. Each portion of the fault is modeled from one slider and the system loaded by a constant force per unit length F. The behavior of the system is determined from the constitutive laws and the equation of force balance on each slider. The displacement of slider i is noted δ_i, its velocity is $V_i = d\delta_i/dt$, and the frictional stress is τ_i. The length of spring i is l_i^0 when the spring is at rest, and its stiffness is noted k_i. The width (or down-dip extent) of each fault zone is noted w_i, i = 1,3. The stiffness k_1 of the SFZ and k_2 of the BCFZ are related to their width w_1 and w_2 through the relation

$$k_i = G/w_i,\ i = 1, 2, \tag{1}$$

where G is the shear modulus.

[5] This simple model is meant to investigate the effect of stress transfer on nonlinear strain buildup in the interseismic period. It does not mean to simulate the full complexity of real faults. The model ignores, in particular, the effect of heterogeneities of frictional properties, fault geometry, or faults interactions in three dimensions that are probably essential to explain some aspects of real fault behavior, including the fact that the return of large earthquake on a given fault is probably not cyclic. Also, we neglect the fact that the viscous behavior of the fault zone is probably non-Newtonian and varies with depth. For these reasons, any direct application of the model to analyze real data should be subject to caution.

2.1. Slider 1: Seismogenic Fault Zone

[6] A rate-and-state friction law is ascribed to slider 1 [*Dieterich*, 1979; *Ruina*, 1983] as often assumed in seismic cycle models [*Rice*, 1993; *Lapusta and Rice*, 2003; *Perfettini et al.*, 2003a, 2003b]. The frictional stress is

$$\tau_1(V_1(t), \theta_1(t)) = \sigma_1 \left[\mu_1^* + a_1 \log\left(V_1(t)/V_*\right) + b_1 \log\left(\theta_1(t)/\theta_*\right)\right], \tag{2}$$

where σ_1, $V_1(t)$, and $\theta_1(t)$ are the normal stress, sliding velocity, and state variable of slider 1 at time t, respectively.

The parameters a_1 and b_1 are empirical constants, while V_1^*, θ_1^*, and μ_1^* are reference values such that $\tau_1(V_1^*, \theta_1^*)/\sigma_1 = \mu_1^*$. The state variable θ_1 follows the Dieterich (aging) law

$$\dot{\theta}_1 = 1 - \frac{V_1(t)\theta_1(t)}{D_c}, \tag{3}$$

where D_c is a characteristic length.

[7] For slip instabilities to be possible, we assume a rate-weakening behavior, i.e., $a_1 < b_1$ [*Rice and Ruina*, 1983]. These are computed from a quasi-dynamic approximation [*Rice*, 1993] by writing

$$\frac{-GV_1}{2\beta} - k_1\left[(\delta_1 - \delta_2) - l_1^0\right] = \tau_1(V_1, \theta_1). \tag{4}$$

The first term is a radiation damping term which prevents infinite velocities during slip instabilities. It depends on the shear modulus G and the shear wave velocity β. We assume $G = 30$ GPa and $\beta = 3$ km/s. When considering spring-slider systems, slip instabilities are usually prevented by including inertial terms [e.g., *Roy and Marone*, 1996]. However, it is very difficult to estimate these terms. On the other end, the existence of the radiation damping term is justified by elastodynamic considerations [see, e.g., *Rice*, 1993]. Anyway, the goal of the SFZ in our model is to transfer stresses "instantaneously" (i.e., duration of the seismic phase much lower than t_r, T_{cycle}, and T_{M}) in the BCFZ and DFZ. We may either use a mass or the radiation damping term to prevent instability.

[8] The stress drop $\Delta\tau$ during each slip event scales as $\Delta\tau \propto \sigma_1(b_1 - a_1)$ [*Rice and Tse*, 1986]. The stiffness k_1 of slider 1 has a moderate influence on the stress drop but determines coseismic slip (see equation (A4))

$$\Delta U = \frac{\Delta\tau}{k_1}. \tag{5}$$

2.2. Slider 2: Brittle Creep Fault Zone

[9] As suggested from experimental results on the effect of temperature on rock friction [*Blanpied et al.*, 1995] and from the common observation of deep afterslip following major earthquakes, the fault zone down dip of the SFZ is assume to undergo rate-strengthening frictional sliding [*Rice*, 1993; *Perfettini and Avouac*, 2004], with the frictional stress being

$$\tau_2(V_2(t)) = \sigma_2\left[\mu_2^* + a_2 \log\left(V_2(t)/V_*\right)\right], \tag{6}$$

where σ_2 and $V_2(t)$ are the normal stress and sliding velocity of slider 2, respectively, while μ_2^* and $a_2 > 0$ are empirical constants. The force balance on slider 2 implies

$$k_1\left[(\delta_1 - \delta_2) - l_1^0\right] - k_2\left[(\delta_2 - \delta_3) - l_2^0\right] = \tau_2(V_2). \tag{7}$$

2.3. Slider 3: Ductile Fault Zone

[10] The shear stress τ_3 acting on slider 3 is computed from

$$\tau_3(V_3) = \eta V_3, \tag{8}$$

where $\eta = \nu/\Delta h$, where ν is the viscosity of the viscous layer and Δh is its thickness. The phase of viscous relaxation is commonly characterized by the Maxwell time defined by

$$T_{\text{M}} = \frac{\eta}{K}, \tag{9}$$

where $K = (w_1/w_3)[k_1k_2/(k_1 + k_2)]$ (see equation (A11)). The force balance on slider 3 implies

$$F = \tau_1(V_1, \theta_1)w_1 + \tau_2(V_2)w_2 + \tau_3(V_3)w_3, \tag{10}$$

F being the loading force per unit length (along the strike of the fault).

2.4. Equations of Motion

[11] The behavior of the spring-slider system is determined from combining the equations above. After a derivation with respect to time of equations (4) and (7), the system of equations (4)–(10) can be written as

$$\frac{dV_1}{dt} = \frac{-k_1(V_1 - V_2) - \dfrac{\sigma_1 b_1}{\theta_1}\dfrac{d\theta_1}{dt}}{\dfrac{\sigma_1 a_1}{V_1} + \dfrac{G}{2\beta}}, \tag{11}$$

where $d\theta_1/dt$ is given by equation (3). For slider 2 we obtain

$$\frac{dV_2}{dt} = \frac{V_2}{\sigma_2 a_2}[k_1(V_1 - V_2) - k_2(V_2 - V_3)], \tag{12}$$

while the sliding velocity of slider 3 is obtained using equations (8) and (10) leading to

$$V_3 = \frac{1}{\eta w_3}[F - (\tau_1 w_1 + \tau_2 w_2)]. \tag{13}$$

The system of equations (11)–(13) is solved using a Runge-Kutta algorithm [*Press et al.*, 1992] with a fifth-order adaptive step-size control.

2.5. Minimum Force F_c for Motion and Long-Term Sliding Velocity V_0

[12] The fault model used in this study requires a driving force larger than some critical value F_c to overcome the frictional resistance to sliding. If the force is less than critical, there is no fault motion and $\tau_3 = 0$.

[13] The average convergence rate across the system can then be estimated approximately by assuming that variations of the stresses τ_1 and τ_2 are small compared to the static values $\tau_1^S = \sigma_1\mu_1^*$ and $\tau_2^S = \sigma_2\mu_2^*$. Indeed, reasonable values of a_1, b_1, and a_2 are usually at least 1 order of magnitude lower than μ_1^* and μ_2^* [*Marone*, 1998]. The average sliding velocity V_0 of the viscous slider can then be obtained using equation (13), leading to

$$V_0 = \frac{1}{\eta w_3}(F - F_c), \tag{14}$$

with

$$F_c \simeq \tau_1^S w_1 + \tau_2^S w_2 = \sigma_1\mu_1^* w_1 + \sigma_2\mu_2^* w_2. \tag{15}$$

Table 1. Parameters Used in This Study

Parameter	Value
μ_1*	0.6
μ_2*	0.6
a_1	0.004
b_1	0.005
D_c	0.01 m
V*	10^{-10} m/s
a_2	0.002
σ_1	270 MPa
σ_2	540 MPa
w_1	20 km
w_2	10 km
w_3	200 km
Δh	5 km

With the set of parameters given in Table 1, the critical force is of the order of $F_c = 6.48 \times 10^{12}$ N/m.

3. Presentation of Numerical Experiments

3.1. Parameters of the Model

[14] We ran several numerical experiments that were meant to reveal the factors controlling temporal variations of strain rate, in particular, the sensitivity to the viscosity ν of the DFZ, which was varied between 10^{18} and 10^{20} Pa s. Other model parameters are listed in Table 1. We did not explore, for example, the effect of the frictional parameters of the SFZ since they primarily determine the coseismic stress drop and the detail of the preseismic and coseismic phases [e.g., *Stuart*, 1988; *Mitsui and Hirahara*, 2001]. The frictional parameters of the SFZ were set to some arbitrary values, in the range of laboratory constraints [*Marone*, 1998]. The chosen set of values corresponds to a coseismic stress drop $\Delta\tau \simeq 8$ MPa and a coseismic slip of the order of 5 m. The maximum slip velocity on the SFZ is of the order of 1 m/s. The parameters of the BCFZ were also not varied and arbitrarily fixed to the values obtained from the analysis of afterslip following the Chi-Chi earthquake [*Perfettini and Avouac*, 2004].

[15] We ran two sets of experiments corresponding to two values of the long-term convergence rate of either 21 mm/yr (a value comparable to the convergence rate across the Nepal Himalaya) or 40 mm/yr (a value comparable to the convergence rate across the western foothill of the central range in Taiwan). For each experiment the value of the driving force was adjusted so as to get the imposed long-term convergence rate using equation (14).

[16] The model predicts a periodic behavior characterized by stress transfers between the three sliders. Figures 2 and 3 show the slip history of all three sliders for two different viscosities corresponding to Maxwell time of 6340 and 63.4 years, respectively. Slider 1 has a stick-slip behavior. Slider 2 produces some afterslip that decays rapidly over the first few years of postseismic relaxation. If the viscosity is high enough, slider 3 has a nearly uniform motion (Figure 2).

3.2. Behavior of the BCFZ

[17] After each slip event along the SFZ the stress level in the BCFZ suddenly increases by some value of the order of the coseismic stress drop $\Delta\tau$ (see equation (A5)). This stress transfer can be considered as almost instantaneous since the characteristic time t_r of the BCFZ is much larger than the duration of the coseismic phase (tens of seconds). The stress

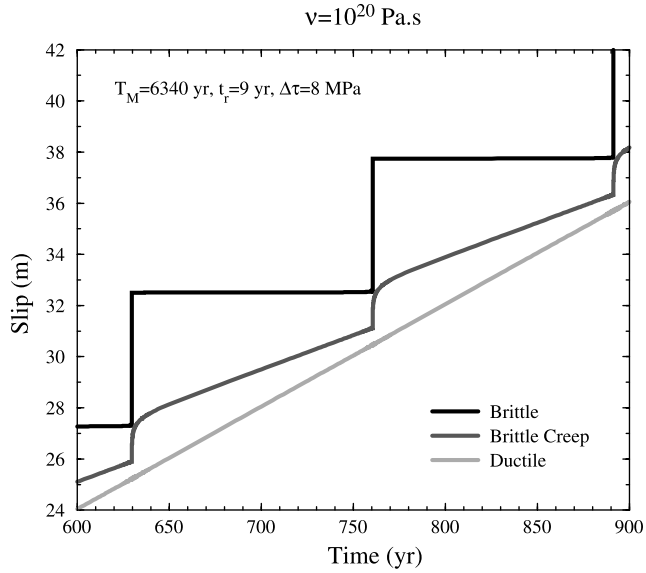

Figure 2. Slip along the SFZ (black line), the BCFZ (dark gray line) and the DFZ (light gray line) during the earthquake cycle. The viscosity is $\nu = 10^{20}$ Pa s, and the loading force is $F = 1.16\ 10^{13}$ N/m, leading to a long-term slip rate $V_0 = 40$ mm/yr and a return period of slip events $T_{\text{cycle}} = 130$ years.

increase induces an abrupt jump of the sliding velocity. According to equation (6) the velocity is increased by a factor $\exp[\Delta\tau/(a_2\sigma_2)]$.

[18] This sudden stress change in the BCFZ is followed by a relaxation phase [*Perfettini and Avouac*, 2004] following some Omori law with a characteristic time t_r of the order of

$$t_r = \frac{a_2\sigma_2}{k_2 V_0}. \tag{16}$$

During this phase, slip on the BCFZ increases logarithmically with time. For a long-term sliding velocity of the

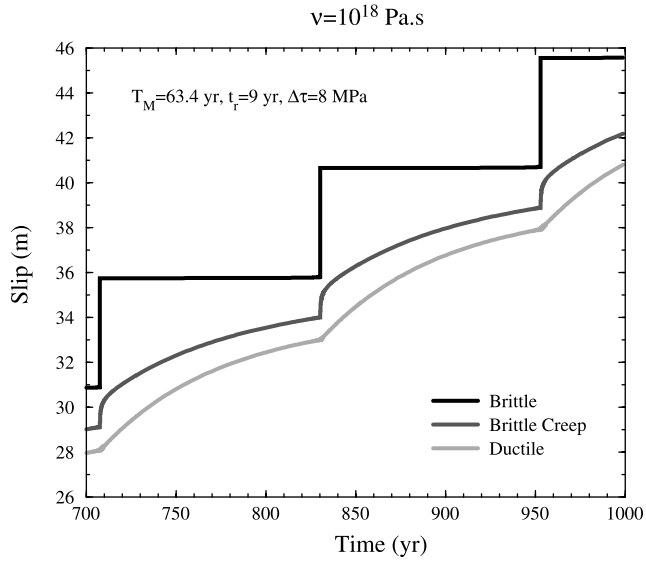

Figure 3. Same as Figure 2 for a viscosity of $\nu = 10^{18}$ Pa s. The loading force $F = 6.55 \times 10^{12}$ N/m was adjusted so as to get the same long-term slip rate $V_0 = 40$ mm/yr.

order of V_0 = 40 mm/yr, equation (16) yields t_r = 9 yr. For the same rheological parameters and an average convergence rate of 21 mm/yr, it yields t_r = 18 years.

[19] After the transient postseismic relaxation driven by its rheological properties the BCFZ continues to slide as a response to loading induced by slip along the DFZ. For a large viscosity ($\nu = 10^{20}$ Pa s), slip of the BCFZ increases nearly linearly with time (Figure 2). At small viscosity ($\nu = 10^{18}$ Pa s), as can be seen on Figure 3, the sliding rate is far from stationary and is dictated by slip along the DFZ according to equation (A2).

3.3. Behavior of the DFZ

[20] For a high viscosity ($\nu = 10^{20}$ Pa s), Figure 2 shows that the sliding velocity of the DFZ is hardly affected by coseismic stress transfer. It always remains close to the long-term average slip rate V_0. This is due to the fact that in that case, the Maxwell time is much larger than the duration of the interseismic period and the stress transferred to the ductile shear zone following the coseismic stress drop is small compared to the driving force. More precisely, in the case of the experiment shown in Figure 2 the coseismic stress drop induces only an increase of the viscous force of $w_1\Delta\tau/(F - F_c) \simeq 0.034$ and the Maxwell time, 6340 years, is much larger than the 130 year return period of coseismic slip. If the viscosity is smaller, the Maxwell time is reduced compared to the duration of the interseismic period. Also the force required to drive the imposed long-term slip rate is reduced so that coseismic stress transfer is proportionally increased. Significant changes of sliding rate are thus observed for a viscosity $\nu = 10^{18}$ Pa s (Figure 3). In that case the sliding velocity of the DFZ, which is noted V_f at the end of the cycle, instantaneously jumps to V_i immediately after the earthquake, and the coseismic stress drop induces a large increase of the viscous force of $w_1\Delta\tau/(F - F_c) \simeq 2.5$. If we note $\Delta\tau^D$ the shear stress change in the DFZ, then according to equation (8),

$$V_i - V_f = \frac{|\Delta\tau^D|}{\eta}. \tag{17}$$

Using equation (A6), we find $|\Delta\tau^D| \simeq \Delta\tau(w_1 - w_2)/w_3$, showing that $|\Delta\tau^D|$ does not depend on the viscosity of the DFZ. Equation (17) thus implies that changes of sliding velocity along the DFZ are enhanced if the viscosity is lower.

3.4. Analytical Approximation of the Ratio V_i/V_f

[21] Figure 4 shows the logarithm of the ratio V_i/V_f as a function of α for a long-term velocity of V_0 = 21 mm/yr (open squares) or V_0 = 40 mm/yr (open circles). The dashed line correspond to the analytical approximation obtained assuming $t_r \ll T_{\text{cycle}}$

$$\log\left(V_i/V_f\right) = \alpha, \tag{18}$$

given in Appendix A, where $\alpha = T_{\text{cycle}}/T_{\text{M}}$. The agreement between the numerical and the analytical results is very good, proving that the dynamic of the DFZ is indeed controlled by the parameter α.

[22] Therefore the ration V_i/V_f only depends on the ratio between the duration of the earthquake cycle and the Maxwell time. Since $T_{\text{cycle}} \simeq \Delta\tau/k_1V_0$ (see equation (A26)) and using equations (A12) and (14), we find

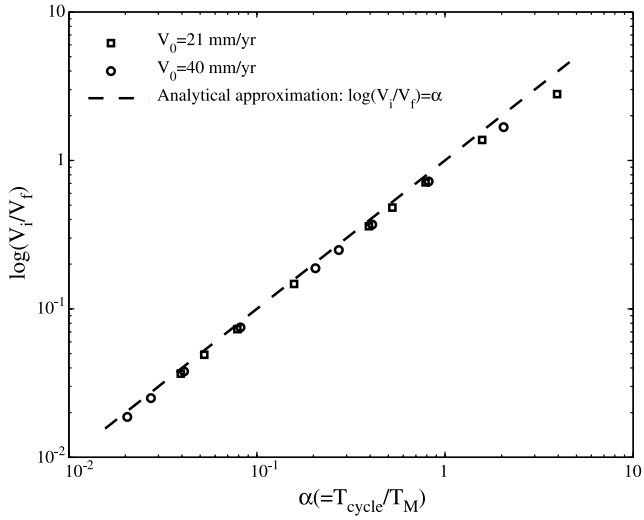

Figure 4. Ratio between the sliding velocity V_i of the DFZ immediately after the earthquake and the sliding velocity V_f immediately before the earthquake as a function of α for a long-term velocity of V_0 = 21 mm/yr (open squares) or V_0 = 40 mm/yr (open circles). The dashed line corresponds to the analytical approximation log $(V_i/V_f) = \alpha$ given in equation (A18).

$$\alpha = \frac{\Delta\tau}{V_0\eta}\frac{K}{k_1} = \frac{k_2}{k_1 + k_2}\frac{w_1\Delta\tau}{F - F_c}, \tag{19}$$

where K is given in equation (A11). Equations (18) and (19) show that the ratio V_i/V_f depends on the geometric factor $k_2/(k_1 + k_2)$ and the ratio between $w_1\Delta\tau$, the force drop associated with coseismic stress drop on the SFZ, and $F - F_c$, the force in excess of the frictional strength of the system. It follows from this simple analysis that the fluctuations of the apparent long-term velocity V_3 are significant when α is large and negligible when α is small.

4. Discussion and Conclusive Remarks

[23] The simple model of the seismic cycle discussed in this paper predicts a periodic cycle with a coseismic phase that depends only on the frictional properties of the SFZ and a postseismic phase driven by a combination of afterslip along the BCFZ (controlled by the frictional properties of that fault portion) and viscous relaxation along the DFZ. Loading of the seismogenic zone in the interseismic period results from elastic stress buildup induced by ductile shear along the DFZ, so that viscosity exerts a key control on the behavior of the system. In particular, it can be easily shown using equation (14) that $T_{\text{cycle}} \propto \eta$ since

$$T_{\text{cycle}} \simeq \Delta\tau/(k_1V_0) = \frac{\eta w_3}{G}\frac{w_1\Delta\tau}{F - F_c}, \tag{20}$$

where equations (A26), (14), and (1) have been used. The response of the BCFZ depends on the frictional parameter $a_2\sigma_2$, the stiffness k_2 of slider 2, and the long-term velocity

Table 2. Effect of an Increase of Viscosity by a Factor β on the Parameters of the Model

η	$\beta\eta$
V_0	$\frac{V_0}{\beta}$
t_r	βt_r
$\Delta\tau$	$\Delta\tau$
ΔU	ΔU
T_{cycle}	βT_{cycle}
T_{M}	βT_{M}
α	α

V_0. From equation (16) we infer that the characteristic time t_r for relaxation of the BCFZ scales as $t_r \propto \eta$ since $V_0 \propto 1/\eta$ (see equation (14)). Table 2 summarizes the effect of an increase of viscosity by a factor β at constant driving force.

[24] This model shares many similarities with spring-slider models obtained by imposing a constant loading velocity. The two approaches are not equivalent if stress transfers during the seismic cycle are significant relative to the average stress level driving tectonic deformation, i.e., if α is large. In that case, the assumption of a constant driving force implies fluctuations of strain rate during the seismic cycle.

[25] In the literature, models of the seismic cycle have put the emphasis either on the frictional properties of the fault zone [e.g., *Rice*, 1993] or the viscous properties of the asthenosphere [e.g., *Thatcher and Rundle*, 1984]. Our model combines the two approaches, assuming that postseismic relaxation, which is governed by rate-strengthening friction, occurs on a characteristic time t_r much smaller than the interval between two recurring large earthquakes. This, and the assumption of a constant driving force, leads to a relaxation process with both afterslip and viscous relaxation. One interesting implication of this model is that the loading velocity should change instantaneously by a factor $V_i/V_f = \exp(\alpha)$ to compensate the coseismic stress drop and then decrease exponentially with time. The 1-D model presented here obviously overestimates the effect that might occur in a real 3-D medium. The coseismic stress changes occur in the 3-D medium surrounding the ruptured fault zone so that the direct effect on the down-dip portions of the fault zone would not be as large as assumed here. However, this would affect the geometric factors that appear in some of the equations obtained in this study, but the principle should still hold.

[26] It is generally admitted that the viscous behavior of rocks is non-Newtonian, and it might therefore be argued that the DFZ might be better described using a nonlinear law $V_3 = C\tau_3^n$, C being a constant and n a stress exponent, greater than 1 and possibly around 3 [see, e.g., *Turcotte and Schubert*, 1982]. In this study we have assumed a Newtonian rheology ($n = 1$). If a non-Newtonian rheology is assumed, the apparent viscosity $\eta = \tau_3/V_3$ scales as $V_3^{1/n-1}$ and becomes rate-dependent. In this case, the discussion of the results becomes more intricate and our model would loose part of its pedagogic virtue. Furthermore, one can easily verify from equation (10) that in the case of a non-Newtonian rheology the fluctuations of the sliding velocity of the DFZ (for a given value of α) would be enhanced (since $n > 1$) compared to the Newtonian case. Therefore our point that fluctuations of the sliding velocity of the DFZ might occur during the earthquake cycle would still hold.

[27] It should be clearly understood that the periodic behavior of the system analyzed here is due to simplifying assumptions which do not apply to real faults. Frictional and material heterogeneities or fault interactions in three dimensions are very likely to induce significant fluctuations of the time interval between two large earthquakes on a given fault. Nevertheless, we believe that the model we propose is the simplest that can be proposed to illustrate the basic concept we wanted to investigate but is far from reproducing the complex behavior of real fault systems. Whether earthquake recurrence on a particular fault is periodic or not, variations of the sliding velocity of the DFZ are expected when α is large, not when α is small. In particular, the analytical derivation presented in section A3 and which leads to $V_i/V_f = \exp(\alpha)$ is only based on the assumption that the time interval between the two successive events is T_{cycle} but makes no assumption about the periodicity of the cycle. Furthermore, equation (19) gives an expression of α that is independent on the duration of the earthquake cycle, removing the assumption of a periodicity of the earthquake cycle.

[28] The model is probably too simple to apply to any particular data set, but we think it provides some insight into the physics of the seismic cycle. It helps in particular to identify some key parameters which might control the time evolution of interseismic strain. Also it implies that there is no necessity that long-term geological slip rates on faults be equal to loading velocities measured at some distance from the fault zone using GPS or other geodetic technique. This may be expected in reality since coseismic stress drop during large earthquakes can typically be of the order of 10 MPa, while deviatoric stresses at seismogenic depth could be as low as a few hundred megapascals. The loading velocity might be either larger or smaller depending on the age of the latest major earthquake on the fault, and the effect should be all the more important if significant stress fluctuations occur during the seismic cycle. The critical factor would then be the ratio between the amplitude of the deviatoric stresses induced by driving tectonic forces and coseismic stress drop, which depends only on the frictional properties of the seismogenic fault zone. The viscosity would then be controlling the time interval between two recurring earthquakes on the same major fault zone as well as the duration of the postseismic relaxation phase.

[29] Future investigations should consider more realistic fault models to assess in particular how the conclusions of this study are affected if stress transfers are computed from a more realistic 3-D model.

Appendix A: Useful Analytical Approximations

[30] We present here some analytical approximations that provide a better understanding of the response of the DFZ to an earthquake in the SFZ.

A1. Relation Between the Sliding Velocity of the BCFZ and DFZ in the Interseismic Phase

[31] The relaxation time of the BCFZ being usually of a few years, we can consider that during most of the interseismic period, the BCFZ is in steady state, i.e., $d\tau_2/dt = 0$.

Noting that $V_1 \simeq 0$ during the interseismic period, we find using equation (7) after a derivation with respect to time

$$-k_1 V_2 - k_2(V_2 - V_3) \simeq \frac{d\tau_2}{dt} \simeq 0. \quad \text{(A1)}$$

Therefore, in the interseismic period the sliding velocity of the BCFZ and the DFZ are related by

$$V_2 = \frac{k_2}{k_1 + k_2} V_3. \quad \text{(A2)}$$

Knowing that the long-term velocity of the DFZ is V_0 given in equation (14), we find that an estimate of the long-term velocity V_0^{BC} of the BCFZ is

$$V_0^{\mathrm{BC}} = \frac{V_0}{1 + \frac{k_1}{k_2}} = \frac{V_0}{1 + \frac{w_2}{w_1}}, \quad \text{(A3)}$$

where the definition of the stiffness (see equation (1)) has been used.

A2. Stress Changes During the Earthquake in the Three Fault Zones

[32] Let us note τ_i^+ (respectively τ_i^-), δ_i^+ (respectively δ_i^-), and V_i^+ (respectively V_i^-), the stress, displacement, and sliding velocity after (respectively before) the earthquake with $i = 1, 3$. Note also that $\delta_2^+ \simeq \delta_2^-$ and $\delta_3^+ \simeq \delta_3^-$ since the displacements of the BCFZ and DFZ do not vary during the event.

[33] Using equation (4), we find

$$-k_1\left(\delta_1^+ - \delta_1^-\right) \simeq \tau_1^+ - \tau_1^-. \quad \text{(A4)}$$

Introducing the static stress drop $\Delta\tau = \tau_1^- - \tau_1^+$ and the coseismic slip $\Delta U = \delta_1^+ - \delta_1^-$, we obtain equation (5).

[34] Similarly, we can use equation (7) to obtain

$$\tau_2^+ - \tau_2^- \simeq k_1\left(\delta_1^+ - \delta_1^-\right) \simeq -\left(\tau_1^+ - \tau_1^-\right) = \Delta\tau. \quad \text{(A5)}$$

In other words, the stress drop of the SFZ due to the earthquake is integrally transferred to the BCFZ.

[35] Finally, equation (10) leads to

$$V_3^+ - V_3^- = V_i - V_f \simeq \left(\frac{w_1 - w_2}{w_3}\right)\frac{\Delta\tau}{\eta}. \quad \text{(A6)}$$

A3. Changes of the Sliding Velocity of the DFZ During the Earthquake

[36] The sliding velocity of the DFZ is suddenly increased because of the earthquake as predicted by equation (A6). Since the characteristic relaxation time t_r of the BCFZ is assumed to be much smaller than the relaxation time of the DFZ, we will assume that the sliding of slider 2 (BCFZ) is steady state. Since $V_1 = 0$ (the fault is locked), we get from equations (4) and (7):

$$-k_2\left[(\delta_2 - \delta_3) - l_2^0\right] = \tau_1 + \tau_2. \quad \text{(A7)}$$

Using equation (A7) together with equation (10) leads to

$$\eta V_3 w_3 = F + \tau_2(w_1 - w_2) + k_2 w_1\left[(\delta_2 - \delta_3) - l_2^0\right], \quad \text{(A8)}$$

which, after derivation with respect to time, yields

$$w_3\eta\frac{dV_3}{dt} \simeq k_2 w_1(V_2 - V_3) \quad \text{(A9)}$$

since we have assumed $d\tau_2/dt \simeq 0$ during the relaxation phase of the DFZ. Using equation (A2), we can rewrite equation (A9) as

$$\frac{dV_3}{dt} \simeq -\frac{K}{\eta}V_3, \quad \text{(A10)}$$

where

$$K = \frac{w_1}{w_3}\frac{k_1 k_2}{k_1 + k_2}. \quad \text{(A11)}$$

We now introduce the Maxwell time

$$T_{\mathrm{M}} = \frac{\eta}{K} = \eta\frac{w_3}{w_1}\left(\frac{1}{k_1} + \frac{1}{k_2}\right). \quad \text{(A12)}$$

With this notation we can integrate equation (A10) with respect to time

$$V_3(t) = V_i \exp\left(-t/T_{\mathrm{M}}\right), \quad \text{(A13)}$$

with the initial condition $V_3(t = 0^+) = V_i$.

[37] Equation (A13) can be used to obtained the velocity V_f of the DFZ immediately before the next event occurring at time T_{cycle}

$$V_f = V_i \exp\left(-T_{\mathrm{cycle}}/T_{\mathrm{M}}\right). \quad \text{(A14)}$$

[38] Combining equations (A6) and (A14) leads to

$$V_i = \frac{1}{1 - \exp(-\alpha)}\left(\frac{w_1 - w_2}{w_3}\right)\frac{\Delta\tau}{\eta}, \quad \text{(A15)}$$

$$V_f = \frac{\exp(-\alpha)}{1 - \exp(-\alpha)}\left(\frac{w_1 - w_2}{w_3}\right)\frac{\Delta\tau}{\eta}, \quad \text{(A16)}$$

where

$$\alpha = \frac{T_{\mathrm{cycle}}}{T_{\mathrm{M}}}, \quad \text{(A17)}$$

while the ratio V_i/V_f yields

$$\frac{V_i}{V_f} = \exp(\alpha). \quad \text{(A18)}$$

A4. Relation Between the Coseismic Stress Drop $\Delta\tau$ and the Duration of the Earthquake Cycle T_{cycle}

[39] The stressing rate on slider 1 may be estimated by taking the derivative of equation (4) with respect to time

$$\dot{\tau}_1 = \frac{-G\dot{V}_1}{2\beta} - k_1(V_1 - V_2), \quad \text{(A19)}$$

where $\dot{(\ )}$ means $d(\ )/dt$. Since $\dot{V}_1 \simeq 0$ and $V_1 \simeq 0$ in the interseismic period, the stressing rate between two earthquakes is given by

$$\dot{\tau}_1 \simeq k_1 V_2. \tag{A20}$$

Equation (A20) may be combined with equation (A7), after a derivation with respect to time, leading to

$$\dot{\tau}_1 \simeq k_1 V_3 - \frac{k_1}{k_2}(\dot{\tau}_1 + \dot{\tau}_2), \tag{A21}$$

which can be rewritten as

$$\dot{\tau}_1 \simeq \frac{k_1 k_2}{k_1 + k_2} V_3 - \frac{k_1}{k_1 + k_2}\dot{\tau}_2. \tag{A22}$$

Once integrated with respect to time, equation (A22) yields

$$\int_0^{T_{\text{cycle}}} \dot{\tau}_1(t')\,dt' \simeq \frac{k_1}{k_1 + k_2}\left[k_2 \int_0^{T_{\text{cycle}}} V_3(t')\,dt' - \int_0^{T_{\text{cycle}}} \dot{\tau}_2(t')\,dt'\right]. \tag{A23}$$

Since V_0 is the average sliding velocity of V_3 over one earthquake cycle, we have

$$\frac{1}{T_{\text{cycle}}} \int_0^{T_{\text{cycle}}} V_3(t')\,dt' = V_0. \tag{A24}$$

Combining equation (A23) together with equation (A24), we obtain

$$\tau_1\left(T_{\text{cycle}}\right) - \tau_1(0) \simeq \frac{k_1}{k_1 + k_2}\left\{k_2 V_0 T_{\text{cycle}} - \left[\tau_2\left(T_{\text{cycle}}\right) - \tau_2(0)\right]\right\}, \tag{A25}$$

which finally leads to

$$\Delta\tau \simeq k_1 V_0 T_{\text{cycle}}, \tag{A26}$$

after use of equation (A5).

[40] Equation (A26) shows that the average stressing rate acting on slider 1 (SFZ) is identical as the one that would be obtained using a single slider (slider 1) under the constant loading velocity V_0, which is the average sliding velocity of the slider 3 (DFZ).

[41] **Acknowledgments.** We are grateful to Massimo Cocco, Teruo Yamashita, and Sandra Stancey for their comments which have been most helpful to improve the manuscript. This is Caltech contribution 9001.

References

Blanpied, M. L., D. A. Lockner, and J. D. Byerlee (1991), Fault stability inferred from granite sliding experiments at hydrothermal conditions, *Geophys. Res. Lett.*, *18*, 609–612.

Blanpied, M. L., D. A. Lockner, and J. D. Byerlee (1995), Frictional slip of granite at hydrothermal conditions, *J. Geophys. Res.*, *100*, 13,045–13,064.

Burridge, R., and L. Knopoff (1967), Model and theoretical seismicity, *Bull. Seismol. Soc. Am.*, *57*, 341–371.

Cattin, R., and J. Avouac (2000), Modeling of mountain building and the seismic cycle in the Himalaya of Nepal, *J. Geophys. Res.*, *105*, 13,389–13,407.

Dieterich, J. H. (1979), Modeling of rock friction: 1. Experimental results and constitutive equations, *J. Geophys. Res.*, *84*, 2161–2168.

Dmowska, R., G. Zheng, and J. Rice (1996), Seismicity and deformation at convergent margins due to heterogeneous coupling, *J. Geophys. Res.*, *101*, 3015–3029.

Lapusta, N., and J. R. Rice (2003), Nucleation and early seismic propagation of small and large events in a crustal earthquake model, *J. Geophys. Res.*, *108*(B4), 2205, doi:10.1029/2001JB000793.

Marone, C. (1998), Laboratory-derived friction laws and their application to seismic faulting, *Annu. Rev. Eath Planet. Sci.*, *26*, 643–696.

Mitsui, N., and K. Hirahara (2001), Viscoelastic simulation of earthquake cycle using a simple spring-dashpot-mass system with a friction law, *Geophys. Res. Lett.*, *28*, 4391–4394.

Perfettini, H., and J.-P. Avouac (2004), Postseismic relaxation driven by brittle creep: A possible mechanism to reconcile geodetic measurements and the decay rate of aftershocks, application to the Chi-Chi earthquake, Taiwan, *J. Geophys. Res.*, *109*, B02304, doi:10.1029/2003JB002488.

Perfettini, H., J. Schmittbuhl, and A. Cochard (2003a), Shear and normal load perturbations on a two-dimensional continuous fault: 1. Static triggering, *J. Geophys. Res.*, *108*(B9), 2408, doi:10.1029/2002JB001804.

Perfettini, H., J. Schmittbuhl, and A. Cochard (2003b), Shear and normal load perturbations on a two-dimensional continuous fault: 2. Dynamic triggering, *J. Geophys. Res.*, *108*(B9), 2409, doi:10.1029/2002JB001805.

Press, W. H., B. P. Flannery, S. A. Teukolsky, and W. T. Vetterling (1992), Integration of ordinary differential equations, in *Numerical Recipes in C, The Art of Scientific Computing*, 2nd ed., pp. 707–752, Cambridge Univ. Press, New York.

Rice, J. R. (1993), Spatio-temporal complexity of slip on a fault, *J. Geophys. Res.*, *98*, 9885–9907.

Rice, J. R., and A. L. Ruina (1983), Stability of steady frictional slipping, *J. Appl. Mech.*, *50*, 343–349.

Rice, J. R., and S. T. Tse (1986), Dynamic motion of a single degree of freedom system following a rate and state dependent friction law, *J. Geophys. Res.*, *91*, 521–530.

Roy, M., and C. Marone (1996), Earthquake nucleation on model faults with rate- and state-dependent friction: Effects of inertia, *J. Geophys. Res.*, *101*, 13,919–13,932.

Ruina, A. L. (1983), Slip instability and state variable fricton laws, *J. Geophys. Res.*, *88*, 10,359–10,370.

Savage, J., and W. Prescott (1978), Astenosphere readjustment and the earthquake cycle, *J. Geophys. Res.*, *83*, 3369–3376.

Scholz, C. H. (1990), *The Mechanics of Earthquakes and Faulting*, Cambridge Univ. Press, New York.

Stuart, W. (1988), Forecast model for great earthquakes at the Nankai through subduction zone, *Pure Appl. Geophys.*, *126*, 619–641.

Thatcher, W., and J. Rundle (1984), A viscoelastic coupling model for the cyclic deformation due to periodically repeated earthquakes at subduction zones, *J. Geophys. Res.*, *89*, 7631–7640.

Tse, S. T., and J. R. Rice (1986), Crustal earthquake instability in relation to the depth variation of frictional slip properties, *J. Geophys. Res.*, *91*, 9452–9472.

Turcotte, D., and G. Schubert (1982), *Geodynamic Applications of Continuum Physics to Geological Problems*, John Wiley, Hoboken, N. J.

Wang, K. (1995), Coupling of tectonic loading and earthquake fault slips at subduction zones, *Pure Appl. Geophys.*, *145*, 537–559.

J.-P. Avouac, Geological and Planetary Sciences, California Institute of Technology, Mail Code 100-23, Pasadena, CA 91125, USA. (avouac@gps.caltech.edu)

H. Perfettini, Institut de Recherche pour le Développement/Laboratoire des Mécanismes de Transferts en Géologie, 38 rue des 36 ponts, F-31400, Toulouse, France. (perfetti@lmtg.ups-tlse.fr)